Journal of Hazardous Materials 198 (2011) 241–246

Contents lists available at SciVerse ScienceDirect

Journal of Hazardous Materials

journal homepage: www.elsevier.com/locate/jhazmat

Hydrous ferric oxide–resin nanocomposites of tunable structure for arsenite removal: Effect of the host pore structure

Jing Wang, Shujuan Zhang, Bingcai Pan*, Weiming Zhang, Lu Lv

State Key Laboratory of Pollution Control and Resource Reuse, School of the Environment, Nanjing University, Nanjing 210093, PR China

ARTICLE INFO

Article history:
Received 20 June 2011
Received in revised form
19 September 2011
Accepted 11 October 2011
Available online 15 October 2011

Keywords:
Nanocomposites
Pore structure
Hydrous ferric oxide
Arsenite removal

ABSTRACT

Hydrous ferric oxide (HFO) loaded hybrid sorbents are considered to be excellent materials for arsenic removal from water. However, role of the host pore structure in the performance of the composites is still unclear. In the current study five HFO nanocomposites of similar HFO loadings (3.9–5.3% in Fe mass) were fabricated for arsenite removal, using self-synthesized polystyrene (PS) resins of similar particle sizes but different pore structures as hosts. Structure analysis demonstrated that the particle size of HFO aggregates decreased with decreasing pore size of PS. The adsorption of arsenite onto the nanocomposites with PS of smaller average pore size achieved equilibrium faster. Analysis of kinetic data with the intraparticle diffusion model demonstrated that arsenite adsorption onto PS–HFO nanocomposites with larger HFO particles was controlled by intraparticle diffusion whereas the limitation caused by intraparticle diffusion was weakened as the particle size of HFO decreased. The adsorption capacity of the hybrid adsorbents increased with decreased pore size of PS. These results indicated that the pore structure of the support materials would play a significant role in the performance of nanoparticle-loaded porous adsorbents.

1. Introduction

Nanosized ferric oxides, such as ferrihydrite [1,2], goethite [3,4], akaganeite [5], hematite [6] and hydrous ferric oxide (HFO) [7], are excellent sorbents for arsenic removal. The size of these ferric oxides is a key factor that influences their adsorption capacity and adsorption affinity [8]. Nanoparticles of smaller size have better performance than their bigger counterparts. For example, a study showed that goethite of 5 nm in diameter can uptake more Hg(II) than that of 25 and 75 nm [8].

However, in practical application these ferric oxide nanoparticles will cause excessive pressure drops and it is hard to separate them from the system [9]. To overcome this bottleneck, research efforts have been made on preparing new hybrid sorbents by loading ferric oxides onto conventional porous sorbents, such as activated carbon [10–13], bead cellulose [14], sand [15], diatomite [16], and polymeric adsorbents [17,18]. To our best knowledge, most of the related studies focused on exploring novel supports for the hybrid sorbents, increasing the loadings of ferric oxides for higher capacity [19], and investigating the effects of different solution chemistry and operating parameters on the performance. The performances of the hybrid sorbents with different porous sorbents as supports vary from each other. The influence may be attributed to the differences in size and shape of the active oxide nanoparticles encapsulated within the porous supports. However, since the chemical environments within the various supports are different, the adsorption affinities are not identical. It is hard to clarify the effects of pore structure of the supports on the adsorption performance by comparison of common adsorption parameters, such as adsorption capacity.

In this study, our efforts were focused on elucidation of the effects of the pore structure of supports on the performance of the hybrid HFO-loaded sorbents. The removal of As(III) by HFO was used to evaluate the performance of the hybrid sorbents, while porous chloromethylated polystyrene (CMPS) resins was selected as the support for HFO loading. CMPS is a macroreticular polystyrene resin adsorbent with some residual chloromethyl groups on its polymeric matrix during the synthetic process. The existence of the residual chloromethyl groups makes the pore structure of the resin adjustable through post-cross-linking [20]. Post-cross-linking usually can increase the specific surface area of the resin while reduce the average pore size. Therefore, through post-cross-linking, resin can provide various host spaces to HFO for the formation of particles in different shapes and sizes while ensure the same chemical environment for the adsorption of As(III) onto HFO. The results are expected to shed some light on the fabrication of hybrid sorbents with tunable particles size and pore structures, and consequently are helpful to obtain materials with optimized performance.

* Corresponding author. Tel.: +86 25 8968 0390.
E-mail address: bcpan@nju.edu.cn (B. Pan).

0304-3894/$ – see front matter © 2011 Elsevier B.V. All rights reserved.
doi:10.1016/j.jhazmat.2011.10.036

2. Materials and methods

2.1. Materials

Ferric chloride hexahydrate, hydrochloride acid, sodium hydroxide, potassium borohydride, potassium hydroxide, and ethanol are of analytical grade and were purchased from Zhongdong Chemical Reagent Co. (Nanjing, China). $NaAsO_2$ (A. R.) was purchased from Aldrich–Sigma (Shanghai, China) and dissolved in deionized water as a stock solution for further use. CMPS resin was purchased from Zhengguang Resin Co. Ltd (Hangzhou, China). The Brunauer–Emmett–Teller (BET) surface area and average pore size of the resin are 39 $m^2\,g^{-1}$ and 29.9 nm, respectively. In addition, the particle size of the resin is 0.6–0.7 mm in diameter.

2.2. Preparation of polysterene (PS) resins

CMPS particles (30 g) were first soaked in nitrobenzene (180 mL) at 298 K in a round bottom flask for over night. Chloride zinc (3–6 g) was then introduced into the mixture as the catalyst for the post-cross-linking reaction. After several hours (0.5–5) of thermal treatment (363–393 K) in an oil bath, the particles were filtered out of the suspension and were extracted with ethanol for 4 h to remove the residual nitrobenzene in the particle pore space. PS resins with different pore structures can be obtained by varying the reaction conditions, such as bath temperature, reaction time, and the dosage of chloride zinc. Higher temperature, longer reaction time and higher dosage of chloride zinc are favorable for the formation of PS resin with larger surface area.

2.3. Preparation of hybrid sorbents

The hybrid sorbents dispersed with HFO particles were fabricated according to the method reported by Pan et al. [21]. In brief, the PS were first soaked with Fe(III) solution and stirred for 24 h. After that the particles were filtered out and stirred in sodium hydroxide solution for another 24 h. HFO nanoparticles were then formed by thermal treatment of the resulting hybrid sorbents at 50 °C for 5 h.

2.4. Characterization

The BET surface area and pore size of the PS were measured using N_2 adsorption and desorption test at 77 K (NOVA3000e, Quantachrome, USA). The HFO particles loaded on PS were observed with transmission electron microscope (Hitachi Model PS-800, Japan). Possible diffraction peaks in HFO sorbents were studied by powder X-ray diffraction patterns over a wide range of angles (5–60°) using a high-resolution X-ray diffractometer (XTRA, Switzerland) with Cu Kα radiation (40 kV, 25 mA).

2.5. Batch sorption experiments

To determine the sorption kinetics, 0.5 g of a given sorbent was introduced to mix with 500 mL solution with 5 mg L^{-1} of arsenite in a 1000 mL flask and stirred at 298 K. At various time intervals 1 mL aliquots were sampled for arsenite analysis. To start the batch sorption runs, 0.05 g of hybrid sorbents were added into 150 mL conical flasks containing 50 mL solution with arsenite concentration ranging from 0 to 50 mg L^{-1}. For the competitive adsorption test, phosphate was employed as a competing ion by introducing certain contents (20 times and 100 times to that of arsenite in moles) of $Na_3PO_4{\cdot}12H_2O$ into the test solution with 0.027 mmol L^{-1} of arsenite. The solution pH was adjusted by sodium hydroxide or hydrochloride to maintain the pH at 7. The flasks were then sealed and shaken in a water-bath shaker at 298 K under 140 rpm for 120 h to ensure equilibrium.

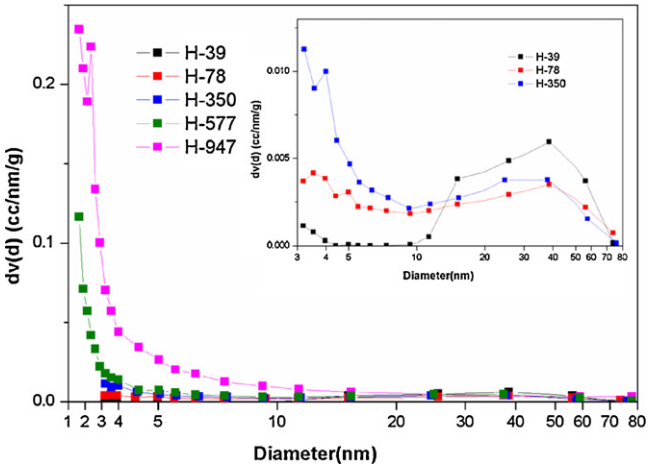

Fig. 1. Pore size distribution of PS resins.

2.6. Analysis

The Fe(III) content in PS–HFO was measured by acid digesting the sorbents and then analyzed by an atomic adsorption spectrometer. Arsenite in solution was determined by using an atomic fluorescence spectrometer with an online hybrid generation unit (model AF-610 A, Rayleigh Instrument Co. Beijing, China). HFO particle size distribution was calculated with a software (Digital Micrograph).

3. Results and discussion

3.1. Characterization of hybrid materials

For the convenience of description, the resins and nanocomposites prepared in this work were denoted as PS-*X* and PS-*X*–HFO, respectively, with X representing the specific surface area of the resin matrix. The pore size distributions of PS-*X* (Fig. 1) indicated that these PS-*X* resins had different pore structures. Pores of diameter less than 3 nm dominate in PS-947 and PS-577, while pores larger than 20 nm dominate in PS-39. The pores in PS-350 and PS-78 had a wide distribution: 27.5%, 18.9% were in the range of 3–20 nm and 72.5%, 81.1% were larger than 20 nm. As shown in Table 1, as the surface area of PS-*X* or PS-*X*–HFO increased, the average pore size decreased. The ΔS/Fe (change of surface area per loading Fe in mass) was calculated to reflect the size of HFO within the hybrid sorbents. A larger ΔS/Fe means smaller HFO particles if the pores were not blocked. As shown in Table 1, ΔS/Fe increased with the surface area of PS-*X* increased up to 350 $m^2\,g^{-1}$, and then deceased as the surface area of PS-*X* further increased to 577 $m^2\,g^{-1}$. A negative ΔS/Fe was observed as the surface area of PS-*X* reached to 947 $m^2\,g^{-1}$. The encapsulation of HFO nanoparticles within the PS led to the reduction in ΔS/Fe due to pore blockage caused by HFO nanoparticles. TEM analysis (Fig. 2a, the TEM result of PS-350–HFO was provided here as a representative) revealed that HFO were well dispersed into the pores of PS as nanoparticles. The size histogram displayed in Fig. 2b indicated that most of the HFO aggregates were between 3 and 7 nm in diameter. XRD spectra of PS-350–HFO showed that the loaded HFO nanoparticles were amorphous, which has been proved to be favorable for arsenite removal [8]. In a word, PS resins with larger surface area and smaller average pore size were better at dispersing the loaded HFO nanoparticles until a critical pore size was reached.

Table 1
Salient properties of PS-*X*–HFO.

Property	BET surface area ($m^2\ g^{-1}$)	Average pore size (nm)	HFO loadings (Fe mass%)	S/Fe ($m^2\ g^{-1}$)
PS-39	39	29.9		
PS-39–HFO	45	25.8	3.9	153.8
PS-78	78	11.6		
PS-78–HFO	88	11.5	4.8	208.3
PS-350	350	4.2		
PS-350–HFO	388	4.0	5.3	717.0
PS-577	577	4.0		
PS-577–HFO	582	3.7	5.2	96.2
PS-947	947	2.5		
PS-947–HFO	859	2.9	4.9	−1795.9

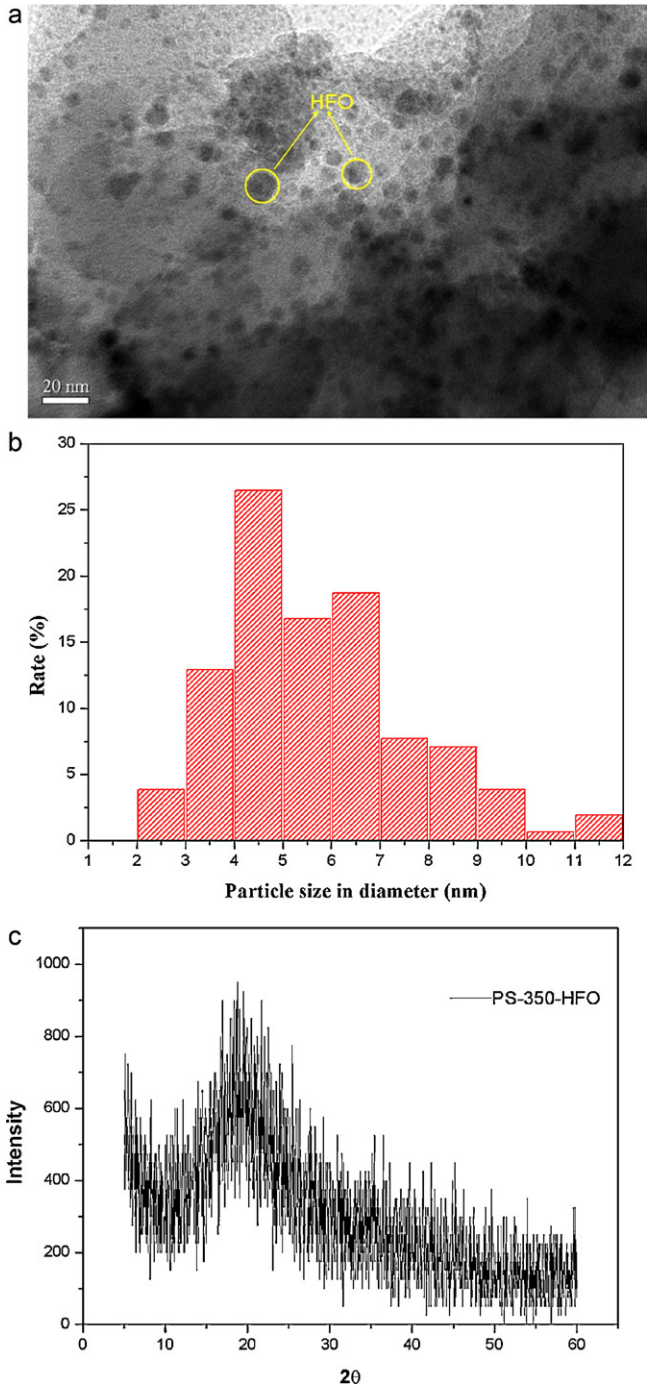

Fig. 2. (a) TEM image of PS-350–HFO, (b) HFO particle size distribution of PS-350–HFO, and (c) XRD pattern of PS-350–HFO.

3.2. Effect of host pore structure on adsorption performance

3.2.1. Adsorption kinetics

Arsenite adsorbs onto HFO by forming inner-sphere surface complex [22,23]. Based on the TEM and SEM images of PS-350–HFO (Figs. 2a and 3a), the arsenite–PS–HFO system is schematically illustrated in Fig. 3b. PS is a netty polymeric sorbent with rigid nano pores [24] and HFO particles were well dispersed in the pore. The HFO nanoparticles were dense aggregates, encapsulating active sites into the multigrain interior interface [8]. Generally, adsorption of arsenic onto HFO loaded hybrid sorbents involved the following steps [25]: (I) bulk diffusion, as for the adsorption onto PS-*X*–HFO, arsenite needs to diffuse across the pore of PS; (II) boundary layer diffusion around HFO particles. In some cases, arsenite adsorbs immediately to the external active sites of HFO particles; (III) intra-particle diffusion within HFO particles; (IV) final equilibrium stage. Fig. 4 presents the plots of arsenite removal versus contact time for all the resulting hybrid sorbents. Adsorption reached equilibrium faster on the hybrid sorbent with larger surface area and smaller average pore size. To determine the rate-limiting step in the sorption process, intra-particle diffusion model (IPD) was employed to simulate the kinetic data [26]:

$$Q_t = K_i t^{0.5} + C \quad (1)$$

where Q_t (mg As g^{-1} resin) is the amount adsorbed at time t (h), K_i is the diffusion rate constant (mg g^{-1} $h^{-0.5}$) and C is the intercept for any experiment. The results are presented in Table 2 and Fig. 5.

A linear plot of Q_t vs. $t^{0.5}$ means that the process was intra-particle diffusion controlled while a multi-linear plot suggests that multiple steps control the process. In the current study, two of the plots (PS-39–HFO and PS-78–HFO) were linear and the other three (PS-350–HFO, PS-577–HFO and PS-947–HFO) were multi-linear (Fig. 5). These results suggested that the HFO particles within a support with lower surface area and larger pores were presented in larger size and had less external active sites. As a result, intra-particle diffusion was the main step that controlled the adsorption process. As the pore size of the support decreased, the HFO particles became smaller. As a consequence, except intraparticle diffusion, the other steps made enhanced contributions to the whole process. Therefore, the Q_t vs. $t^{0.5}$ plot was multi-linear. The relative contributions of initial adsorption and boundary layer diffusion were reflected by the intercept C. A positive C means there is a fast initial

Table 2
Intra-particle diffusion model parameters of arsenite sorption onto PS-*X*–HFO at 298 K.

	K_1	R^2	I	K_2	R^2	K_3	R^2
PS-38–HFO	0.35	0.983	−0.223				
PS-78–HFO	0.37	0.987	−0.037				
PS-350–HFO	0.70	0.990	−0.273	0.27	0.983		
PS-577–HFO	0.77	0.987	−0.115	0.30	0.982	0.174	0.971
PS–947–HFO	1.14	0.994	0.061	0.45	0.979	0.08	0.961

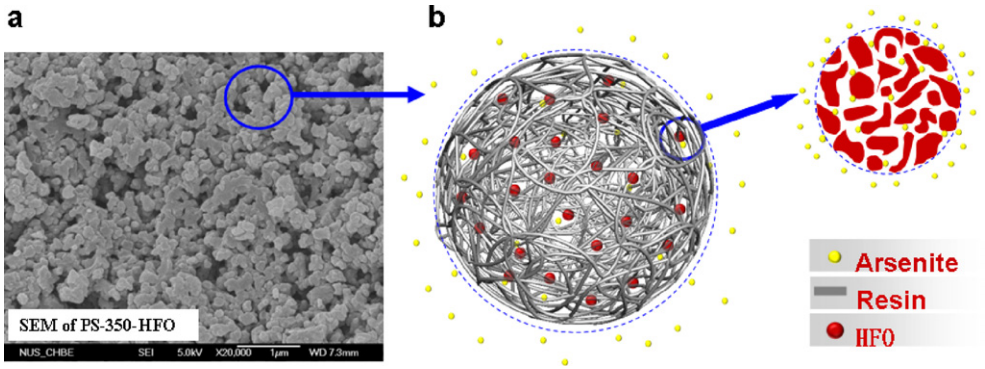

Fig. 3. (a) SEM image of PS-350–HFO, (b) schematic illustration of arsenite–PS–HFO system.

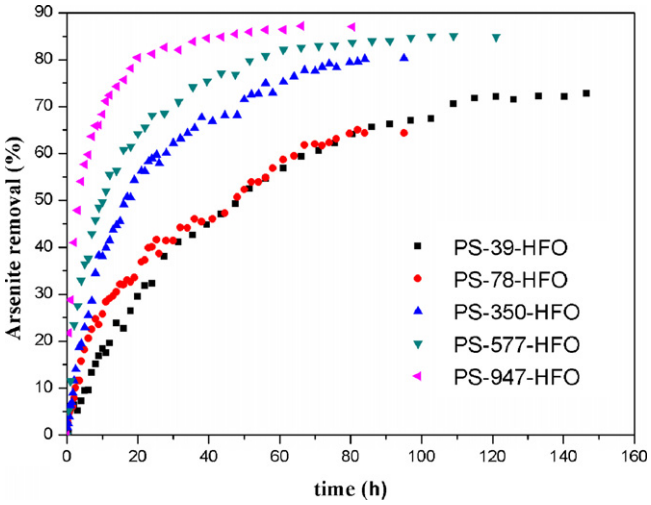

Fig. 4. Plots of arsenite removal versus contact time for PS-X–HFO at 298 K.

adsorption and a negative *C* means there is a delay of adsorption due to boundary later effect [27]. The intercept of the plot for PS-947–HFO was positive whereas those of the other four composites were negative, which further confirmed that PS resins with larger surface area and smaller average pore size were better at dispersing the loaded HFO nanoparticles until a critical pore size was reached. HFO particles of smaller size had more external active sites for the adsorption of arsenite to occur immediately after contact with the sorbent before the occurrence of intraparticle diffusion.

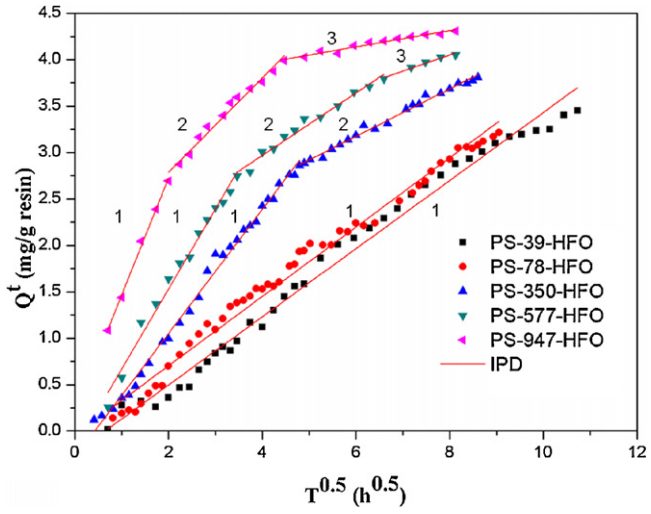

Fig. 5. Intraparticle diffusion plots for the adsorption of arsenite onto PS-X–HFO at 298 K.

3.2.2. *Adsorption isotherms*

Adsorption isotherm experiments of arsenite onto all the hybrid sorbents were conducted at 298 K, and the results are illustrated in Fig. 6. As well-known, adsorption capacity is an important parameter in estimating the performance of sorbents. In Fig. 6, the

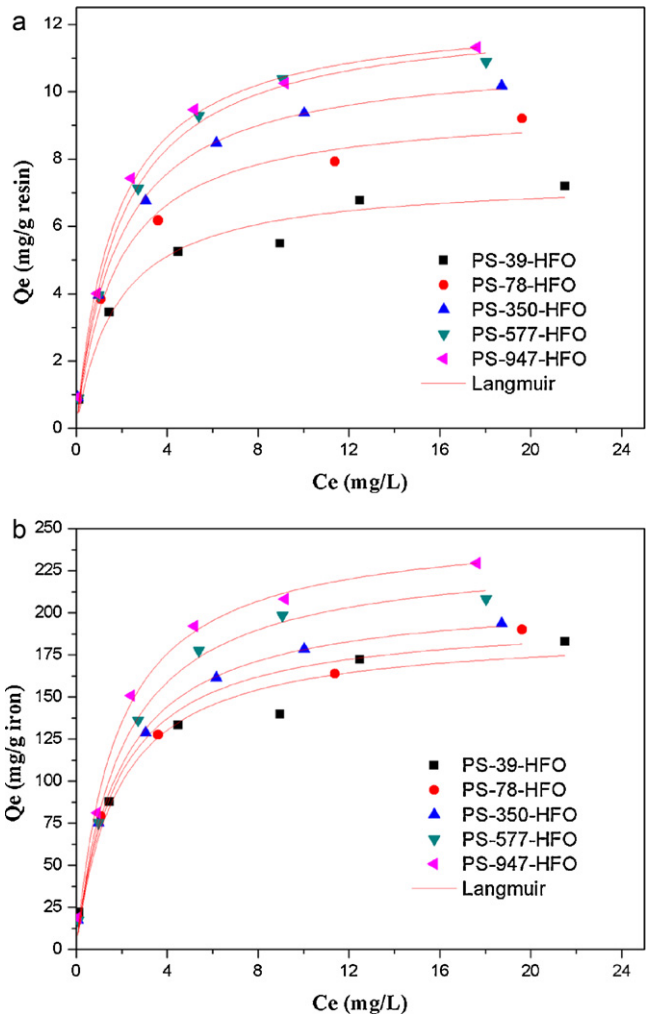

Fig. 6. Adsorption isotherms of arsenite onto PS-*X*–HFO at 298 K (resin dosage: 1.0 g L^{-1}, initial arsenite concentration: 0–50 mg L^{-1}, contact time: 120 h). (a) Adsorption capacity based on mass of resin, (b) adsorption capacity based on mass of iron.

Table 3
Comparison of the performances of arsenite adsorption onto HFO-loaded hybrid sorbents with different supports.

Supports	Fe content (%)	Surface Area ($m^2\ g^{-1}$)	Adsorption Capacity ($mg\ g^{-1}$)	As/Fe (mol/mol)	Ref.
AC	11.7	723	51.3	0.33	[29]
Cellulose	46.8	/	99.6	0.16	[14]
PS-350–HFO	5.3	350	11.08	0.16	This study
Diatomite	25	62.3	29.97	0.09	[16]
Chitosan	8.4	/	6.48	0.06	[30]
Sponge	12	0.022	3.85	0.02	[31]

adsorption capacity was expressed based on the mass of both the hybrid sorbent and the loaded iron to estimate the effects of PS pore structure on the performance of hybrid sorbents.

The Langmuir equation was used to fit the sorption data:

$$\frac{1}{Q_e} = \frac{1}{K_L Q_m C_e} + \frac{1}{Q_m} \quad (2)$$

where C_e is the equilibrium concentration of arsenite in solution ($mg\ L^{-1}$); Q_e is the amount adsorbed at equilibrium concentration ($mg\ g^{-1}$); Q_m is the maximal adsorption capacity ($mg\ g^{-1}$); and K_L is a binding constant.

The Q_m values indicated that arsenite adsorption capacity on HFO was slightly improved as the surface area of PS increased. According to previous study, nanosized ferric oxides with smaller size always have larger surface areas which provide more surface sites at edges or corners and enhance the affinity between ferric oxides and target pollutants [28]. The enhanced Q_m demonstrated that the pore structure of PS controlled the size of HFO nanoparticles, and consequently influenced the adsorption performance of their hybrid composites.

Additionally, the results were compared (Table 3) with previous studies where arsenite sorption were conducted by HFO-loaded hybrid sorbents with different supports, including activated carbon [29], cellulose [14], diatomite [16], chitosan [30] and sponge [31]. Though the surface area values of cellulose and chitosan were not available in ref. [14,30], we might use the reference values of both supports, i.e., 300-600 $m^2\ g^{-1}$ for cellulose [32], and 2-30 $m^2\ g^{-1}$ for chitosan [33], for a simple comparison purpose. It is clear that there is some relevance between the surface area of the support and the arsenite uptake of the hybrid adsorbent. Generally, the adsorption capacity based on loaded iron was improved as the surface area of host increased. It inspired us to study the effects of host pore structure on the performance of HFO-loaded nanocomposites.

3.2.3. Sorption selectivity

In groundwater many anionic components exist other than arsenite, such as phosphates, silicate and sulfate, which could compete with arsenite during the treatment. The ability to resist competitive anions is important in terms of practical application of hybrid sorbents. Here, the competitive adsorption experiment was conducted by introducing phosphate as a competitive anion for arsenite removal to further elucidate the effects of support pore structure on the performance of hybrid sorbents. Phosphate can form strong inner-sphere complex and compete for adsorption sites with arsenite [34,35]. As shown in Fig. 7, phosphate has a significant influence on arsenite adsorption onto the hybrid sorbents. The ability of the hybrid sorbents to resist phosphate was enhanced with the increase of surface area (with PS-947–HFO as an exception), suggesting that HFO particles of smaller size had relatively stronger adsorption affinity to arsenite than to phosphate. The exception of PS-947–HFO reconfirmed that there might exist a critical pore size for HFO. As aforementioned, the $\Delta S/Fe$ values for all other four PS-*X*–HFO were positive while that of PS-947–HFO was negative, because the pores in PS-947–HFO were too small to allow the entrance of HFO particles into them. As a result, compared with the other PS-*X*, more HFO nanoparticles dispersed at the exterior

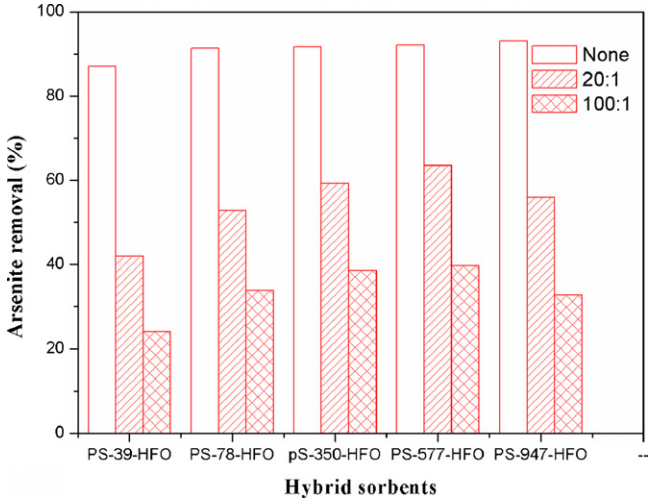

Fig. 7. Effects of phosphate on arsenite adsorption onto PS-*X*–HFO at 298 K. The concentration of phosphate was 20 and 100 times to that of arsenite in mole ratio.

part of PS-947, which led to the positive intercept of Q_t vs. $t^{0.5}$ plot and might be the reason for the weak resistance to competitive irons. Further research is warranted to clarify this point.

4. Conclusions

In the current study, several HFO-loaded PS with different pore structures were prepared and evaluated by arsenite sorption to elucidate the effects of pore structure of PS on controlling HFO particle size and the performance of the hybrid sorbents. Experimental results indicated that HFO nanoparticles can be well restricted in size by controlling the pore structure of the support. The performance of the hybrid sorbents was greatly influenced by the pore structure. In general, PS–HFO with larger surface areas and smaller average pore sizes had faster adsorption kinetics, due to the formation of smaller HFO nanoparticles which possess more exterior active sites. Additionally, the adsorption capacity was slightly improved and the ability to resist competition anion was enhanced to some extent as the surface area of PS increased. The results may serve as guidelines for preparation of hybrid sorbents with tunable structures.

Acknowledgements

The study was supported by NSFC (21177059/51078179), Jiangsu NSF (BK2009253), and the Ministry of Education of China (200802840034).

References

[1] A. Jain, R.H. Loeppert, Effect of competing anions on the adsorption of arsenate and arsenite by ferrihydrite, J. Environ. Qual. 29 (2000) 1422–1430.
[2] K.P. Raven, A. Jain, R.H. Loeppert, Arsenite and arsenate adsorption on ferrihydrite: kinetics equilibrium, and adsorption envelopes, Environ. Sci. Technol. 32 (1998) 344–349.

[3] S. Dixit, J.G. Hering, Comparison of arsenic(V) and arsenic(III) sorption onto iron oxide minerals: Implications for arsenic mobility, Environ. Sci. Technol. 37 (2003) 4182–4189.
[4] J. Gimenez, M. Martinez, J. de Pablo, M. Rovira, L. Duro, Arsenic sorption onto natural hematite, magnetite, and goethite, J. Hazard. Mater. 141 (2007) 575–580.
[5] E.A. Deliyanni, D.N. Bakoyannakis, A.I. Zouboulis, K.A. Matis, Sorption of As(V) ions by akaganeite-type nanocrystals, Chemosphere 50 (2003) 155–163.
[6] J. Gimenez, J. de Pablo, M. Martinez, M. Rovira, C. Valderrama, Reactive transport of arsenic(III) and arsenic(V) on natural hematite: experimental and modeling, J. Colloid Interface Sci. 348 (2010) 293–297.
[7] X.H. Guan, J.M. Wang, C.C. Chusuei, Removal of arsenic from water using granular ferric hydroxide: macroscopic and microscopic studies, J. Hazard. Mater. 156 (2008) 178–185.
[8] G.A. Waychunas, C.S. Kim, J.F. Banfield, Nanoparticulate iron oxide minerals in soils and sediments: unique properties and contaminant scavenging mechanisms, J. Nanopart. Res. 7 (2005) 409–433.
[9] Q.R. Zhang, B.C. Pan, B.J. Pan, W.M. Zhang, K. Jia, Q.X. Zhang, Selective sorption of lead, cadmium and zinc ions by a polymeric cation exchanger containing nano-$Zr(HPO_3S)_2$, Environ. Sci. Technol. 42 (2008) 4140–4145.
[10] Z.M. Gu, J. Fang, B.L. Deng, Preparation and evaluation of GAC-based iron-containing adsorbents for arsenic removal, Environ. Sci. Technol. 39 (2005) 3833–3843.
[11] M. Jang, W.F. Chen, F.S. Cannon, Preloading hydrous ferric oxide into granular activated carbon for arsenic removal, Environ. Sci. Technol. 42 (2008) 3369–3374.
[12] G. Muniz, V. Fierro, A. Celzard, G. Furdin, G. Gonzalez-Sanchez, M.L. Ballinas, Synthesis, characterization and performance in arsenic removal of iron-doped activated carbons prepared by impregnation with Fe(III) and Fe(II), J. Hazard. Mater. 165 (2009) 893–902.
[13] V. Fierro, G. Muniz, G. Gonzalez-Sanchez, M.L. Ballinas, A. Celzard, Arsenic removal by iron-doped activated carbons prepared by ferric chloride forced hydrolysis, J. Hazard. Mater. 168 (2009) 430–437.
[14] X.J. Guo, F.H. Chen, Removal of arsenic by bead cellulose loaded with iron oxyhydroxide from groundwater, Environ. Sci. Technol. 39 (2005) 6808–6818.
[15] V.K. Gupta, V.K. Saini, N. Jain, Adsorption of As(III) from aqueous solutions by iron oxide-coated sand, J. Colloid Interface Sci. 288 (2005) 55–60.
[16] M. Jang, S.H. Min, J.K. Park, E.J. Tlachac, Hydrous ferric oxide incorporated diatomite for remediation of arsenic contaminated groundwater, Environ. Sci. Technol. 41 (2007) 3322–3328.
[17] L. Cumbal, J. Greenleaf, D. Leun, A.K. SenGupta, Polymer supported inorganic nanoparticles: characterization and environmental applications, React. Funct. Polym. 54 (2003) 167–180.
[18] C.M. Iesan, C. Capat, F. Ruta, I. Udrea, Evaluation of a novel hybrid inorganic/organic polymer type material in the arsenic removal process from drinking water, Water Res. 42 (2008) 4327–4333.
[19] Q.J. Zhang, B.C. Pan, W.M. Zhang, B.J. Pan, Q.X. Zhang, H.Q. Ren, Arsenate removal from aqueous media by nanosized hydrated ferric oxide (HFO)-loaded polymeric sorbents: effect of HFO loadings, Ind. Eng. Chem. Res. 47 (2008) 3957–3962.
[20] B.C. Pan, W. Du, W.M. Zhang, X. Zhang, Q.R. Zhang, B.J. Pan, L. Lv, Q.X. Zhang, J.L. Chen, Improved adsorption of 4-nitrophenol onto a novel hyper-cross-linked polymer, Environ. Sci. Technol. 41 (2007) 5057–5062.
[21] B.C. Pan, X.Q. Chen, W.M. Zhang, A process to prepared a polymer-based hybrid sorbent for arsenic removal, Chinese Patent No. ZL200510095177.5, 2005.
[22] D.G. Strawn, A.M. Scheidegger, D.L. Sparks, Kinetics and mechanisms of Pb(II) sorption and desorption at the aluminum oxide water interface, Environ. Sci. Technol. 32 (1998) 2596–2601.
[23] A.C. Scheinost, S. Abend, K.I. Pandya, D.L. Sparks, Kinetic controls on Cu and Pb sorption by ferrihydrite, Environ. Sci. Technol. 35 (2001) 1090–1096.
[24] B.J. Pan, H. Qiu, B.C. Pan, G.Z. Nie, L.L. Xiao, L. Lv, W.M. Zhang, Q.X. Zhang, S.R. Zheng, Highly efficient removal of heavy metals by polymer-supported nanosized hydrated Fe(III) oxides: behavior and XPS study, Water Res. 44 (2010) 815–824.
[25] Q.Y. Sun, L.Z. Yang, The adsorption of basic dyes from aqueous solution on modified peat-resin particle, Water Res. 37 (2003) 1535–1544.
[26] M.S. Bilgili, Adsorption of 4-chlorophenol from aqueous solutions by xad-4 resin: isotherm, kinetic, and thermodynamic analysis, J. Hazard. Mater. 137 (2006) 157–164.
[27] F.C. Wu, R.L. Tseng, R.S. Juang, Initial behavior of intraparticle diffusion model used in the description of adsorption kinetics, Chem. Eng. J. 153 (2009) 1–8.
[28] H. Zeng, A. Singh, S. Basak, K.U. Ulrich, M. Sahu, P. Biswas, J.G. Catalano, D.E. Giammar, Nanoscale size effects on uranium(VI) adsorption to hematite, Environ. Sci. Technol. 43 (2009) 1373–1378.
[29] W. Chen, R. Parette, J. Zou, F.S. Cannon, B.A. Dempsey, Arsenic removal by iron-modified activated carbon, Water Res. 41 (2007) 1851–1858.
[30] D.D. Gang, B. Deng, L. Lin, As(III) removal using an iron-impregnated chitosan sorbent, J. Hazard. Mater. 182 (2010) 156–161.
[31] T.V. Nguyen, S. Vigneswaran, H.H. Ngo, J. Kandasamy, Arsenic removal by iron oxide coated sponge: experimental performance and mathematical models, J. Hazard. Mater. 182 (2010) 723–729.
[32] R.J. Moon, A. Martini, J. Nairn, J. Simonsen, J. Youngblood, Cellulose nanomaterials review: structure properties and nanocomposites, Chem. Soc. Rev. 40 (2011) 3941–3994.
[33] E. Guibal, Interactions of metal ions with chitosan-based sorbents: a review, Sep. Purif. Technol. 38 (2004) 43–74.
[34] Y. Gao, A. Mucci, Acid base reactions, phosphate and arsenate complexation, and their competitive adsorption at the surface of goethite in 0.7 M NaCl solution, Geochim. Cosmochim. Acta 65 (2001) 2361–2378.
[35] Y. Gao, R. Wahi, A.T. Kan, J.C. Falkner, V.L. Colvin, A.B. Tomson, Adsorption of cadmium on anatase nanoparticles-effect of crystal size and pH, Langmuir 20 (2004) 9585–9593.